JOURNAL OF Materials CHEMISTRY

Sonochemical process for the preparation of α-CuSe nanocrystals and flakes†

Hong-Liang Li,[a] Ying-Chun Zhu,[a] Sigalit Avivi,[a] Oleg Palchik,[a] Jin-ping Xiong,[a] Yuri Koltypin,[a] V. Palchik[b] and Aharon Gedanken*[a]

[a] *Department of Chemistry, Bar-Ilan University, Ramat-Gan 52900, Israel.*
E-mail: gedanken@mail.biu.ac.il; Fax: 972-3-5351250; Tel: 972-3-5318315
[b] *Department of Electronics, Jerusalem College of Technology, Jerusalem 91160, Israel*

Received 27th June 2002, Accepted 30th August 2002
First published as an Advance Article on the web 27th September 2002

α-CuSe crystals of different sizes and shapes have been synthesized by a sonochemical method using the less hazardous elemental Se and $Cu(Ac)_2$ as precursors under an atmosphere of H_2/Ar (5 : 95 v/v). X-ray diffraction (XRD), energy-dispersive analytical X-ray (EDAX) and inductively coupled plasma (ICP) have been applied to characterize the products. Transmission electron microscopy (TEM) and selected area electron diffraction (SAED) results show that they are crystallized nanoparticles of tens of nanometers or flakes of 1 μm, depending on the irradiation time. Thermogravimetric analysis (TGA) indicates that the products are stable up to about 480 °C. Diffusion reflection spectra (DRS) reveal that both of them show an indirect band gap with a similar value of about 1.31 eV. Photoacoustic spectra results show that the nanoparticles and the flakes have direct band gaps of about 2.39 eV and 2.21 eV, respectively. This is the first report of the optical properties of α-CuSe. We propose an *in situ* reduction/reaction mechanism to explain the formation of CuSe. The influence of ultrasound on the shape and the size of the product is discussed. The chelating role of the DMSO solvent in the reaction has also been studied.

1 Introduction

Extensive attention has been paid to the preparation and characterization of metal chalcogenides owing to their interesting properties and potential applications.[1–7] Recently, a wide range of techniques has been developed to synthesize metal chalcogenides with control of the microstructure and particle size. These developments include self-propagating high temperature synthesis (SHS),[8] molecular precursor reactions (involving either the thermal decomposition of compounds containing M–S or M–Se bonds or H_2E (E = S, Se) as the chalcogen source),[9,10] and the use of a template agent that utilizes restrictive environments, such as polymer, micelles, zeolites and glass.[11–14] Much of the work has been focused on the formation of controllable nanoparticulate chalcogenides (especially PbS, PbSe, CdS, and CdSe).[15] These nanoparticulates exhibit a size quantization effect that has a potential use for optical signal processors and switches. Other research has shown that solid state metathesis (SSM) reactions can be utilized for the preparation of metal chalcogenides by treating alkali-metal sulfides with metal halides.[16]

The traditional methods, and most of the recently developed methods, usually demand high temperatures, and/or high pressures, toxic precursors, and special matrices. It is difficult to grow well-crystallized nanoparticles under such conditions.

Very recently, Parkin and coworkers[17] reported a route to selenides by a reaction of Se with elemental metals in amine solutions. Subsequently, several improved wet chemical methods were suggested by Qian *et al.*[18–21] to prepare later transition metals and many main-group metal sulfides and selenides. However, some of these approaches need special containers and/or high pressure, corrosive solvents (ethylenediamine) and/or chelating agents, and long reaction times.

Copper selenides in different stoichiometries are semiconductors with *p*-type conductivity, and have been widely used in solar cells,[22] as optical filters,[23] and as superionic materials.[24] Traditionally, bulk copper selenide can be prepared by heating Cu and Se powders at high temperature in flowing Ar.[25] It has also been shown that the element reaction could be promoted by a high-energy milling at room temperature.[26] However, the quality of the product is difficult to control.

All of the new methods produce small nanoparticles, which are useful for optical signal processors and switches. However, large-size copper selenide particles with excellent crystal quality are required for the application of solar cell materials in order to result in a high mobility-life product.[27] Comparing them with other promising metallic selenides, copper selenides have more stoichiometries and phases.[28] Different compositions, stoichiometric (α-Cu_2Se, Cu_3Se, CuSe and $CuSe_2$) and non-stoichiometric ($Cu_{2-x}Se$) and structural forms of them are well-documented.[29] It has been reported that the thermal stability and the band gaps of copper selenides vary depending on their stoichiometries or phases.[30,31] The composition and the crystal structure of the final products are usually dependent on the preparation methods.[18,32–34] However, the preparation methods and size or shape control are less flexible than other metal selenides such as CdSe, and the studies relating to their optical properties are limited. Therefore, to develop new methods for preparing high quality copper selenide crystals and to achieve control of their size or shape are very necessary. Moreover, further studies of their optical properties will help us to understand their interband properties.

Obtaining novel materials with controlled size or shape under mild conditions and with safe precursors at lower temperatures is an issue that has engaged many researchers. Sonic energy has been routinely used in the field of material science for many years.[35,36] Its chemical effects have recently come under investigation for the acceleration of chemical

---

†Electronic supplementary information (ESI) available: EDAX pattern showing Se and Cu signals (Fig. S1), TGA curve of sample I (Fig. S2) and DRS of samples I and III (Fig. S3). See http://www.rsc.org/suppdata/jm/b2/b206193g/

DOI: 10.1039/b206193g

reactions and for the synthesis of new materials, as well as for the generation of novel materials with unusual properties.[37–41]

Herein, we report on a new sonochemical process for the preparation of hexagonal α-CuSe crystals. The new sonochemical method does not need any chelating agent or additive. Simple precursors, elemental Se and $Cu(Ac)_2$, have been utilized. On the other hand, α-CuSe crystals with sizes varying from nanoparticles of tens of nanometers to flakes of 1 μm have been prepared for the first time by the sonochemical process. The thermal stability and optical properties of the particles have been studied. The reaction mechanism and the size control mechanism are also briefly discussed in this paper.

2 Experimental section

$Cu(Ac)_2$, elemental Se ($\sim$100 mesh) and anhydrous dimethyl sulfoxide (DMSO) were purchased from Aldrich and used without further purification. Ultrasonic irradiation was achieved with a high-intensity ultrasonic probe (Misonix; XL sonifier, 1.13 cm diameter Ti horn, 20 kHZ, 60 W cm^{-2} measured calorimetrically).

The X-ray diffraction (XRD) patterns were recorded on a Rigaku X-ray diffractometer (model-2028, Co Kα λ = 1.78892 Å). Morphology and structure investigations were performed with a JEOL-JEM 100SX transmission electron microscope (TEM). Energy-dispersive analytical X-ray (EDAX) was detected on a JEOL-JSM-840 scanning microscope. An inductively coupled plasma atomic emission spectrometer (ICP-AES) model "Spectroflame Modula E" from Spectro, Kleve, Germany, with a standard cross-flow nebulizer, was used to carry out the ICP measurements. Samples were dissolved in dilute nitric acid. Analysis was conducted of portions of these solution, *vs.* certified standards from Merck, by ICP-AES. Thermogravimetric analysis (TGA) was carried out on a Mettler TGA/STDA 851 thermogravimeter analyzer under an Ar atmosphere in the temperature range from 25 to 1000 °C at 10 °C min^{-1}. UV–Vis diffuse reflectance spectroscopy (DRS) was measured by a Cary 500 UV–Visible spectrophotometer at room temperature in the wavelength region between 200 and 800 nm. Photoacoustic measurements were conducted employing a homemade instrument that has been described elsewhere.[42] The value of the band gap was calculated using the "knee method".[43] The powder was diluted with MgO powder in order to prevent saturation phenomenon during photoacoustic measurements (a 5% mixture of CuSe was used).

In a typical procedure, 0.538 g of $Cu(Ac)_2$ and 0.234 g of elemental Se were dispersed in 80 mL DMSO. The mixtures were then irradiated for 1.0, 2.0, and 2.5 h under an H_2/Ar atmosphere at room temperature, and the corresponding as-prepared solids are designated as sample I, sample II and sample III, respectively. During irradiation, the temperature of the solution rose to about 130 °C. After irradiation, the resulting black suspensions were centrifuged and the precipitates were washed three times with absolute ethanol. The solids were dried under vacuum at room temperature for 6 h. To study the reaction mechanism, two control experiments were carried out: (1) $Cu(Ac)_2$ in DMSO was irradiated for 0.5 h, yielding a dark gray precipitate; (2) the resulting solid from (1) was mixed with elemental Se in DMSO solvent, and the mixture was irradiated for 2 h under an H_2/Ar atmosphere. The solids obtained at the end of the control experiments were characterized by means of FTIR and XRD.

3 Results and discussion

3.1 XRD studies

Fig. 1 presents the typical XRD patterns of samples I and III, which can be attributed to the characteristic pattern of α-CuSe.

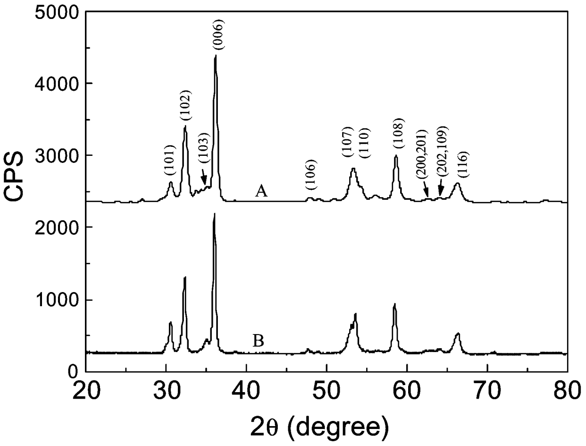

Fig. 1 XRD patterns of samples I (curve A) and III (curve B).

Sample II shows a pattern similar to the above ones (not included in the figure). The main diffraction peaks correspond to the (101), (102), (006), (107), (110), (108), and (116) planes of hexagonal α-CuSe (JCPDS file No. 6-427). After refinement, the cell constants were calculated to be $a = b = 3.952$ Å and $c = 17.356$ Å, which are consistent with the reported data in PDF NO. 6-427. Although there are more than 8 stoichiometries of copper selenides, and some stoichiometries have different phases, each of them has its characteristic XRD pattern.[28] Therefore, the XRD patterns give the most positive evidence of the formation of α-CuSe. The XRD of the product of the first step of the control experiment did not show the presence of elemental Cu (JCPDS file No. 4-836) or of copper oxide (Fig. 2A). The product of the second step was identified as α-CuSe (Fig. 2B). The control experiment results will help us to understand the reaction mechanism in section 3.6.

3.2 EDAX and ICP results

In order to give further evidence to the composition information of the product, EDAX and ICP measurements were performed to detect the ratio of the elements. The EDAX pattern shows very intense Se and Cu signals, which gives an atomic ratio for Cu : Se of 51.6 : 48.4 (see ESI Fig. S1†). It is close to a 1 : 1 stoichiometry. ICP analysis was performed on the copper selenide samples to confirm the stoichiometry. The weight percentages of Cu and Se were 45 and 54, respectively. The weight ratio yields an atomic ratio of Cu : Se of 1.04 : 1. This result further supports the 1 : 1 stoichiometry of CuSe as shown by EDAX analysis.

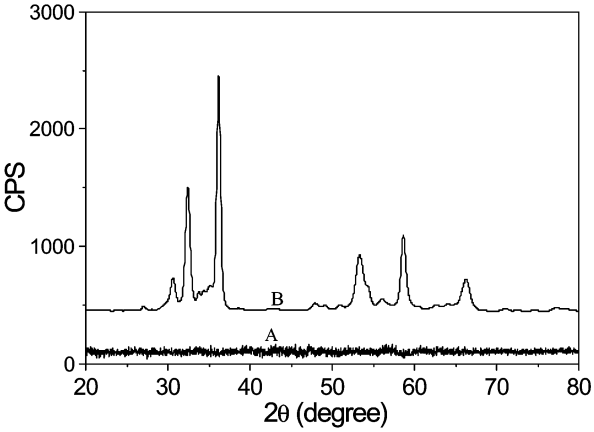

Fig. 2 XRD patterns of the solids after the control experiments (A, the first step; B, the second step).

3.3 TEM results

The morphologies of samples I, II, and III were characterized by TEM. The images and the corresponding selected area diffraction (SAED) patterns are shown in Fig. 3. From the pictures, we can see that the particles prepared with a time of 1.0 h are nearly spherical nanoparticles with diameters in the range 10–20 nm, while the particles obtained with an irradiation time of 2.0 h are flakes with sizes ranging between 200 and 800 nm. Sample III also shows flake morphology with a size value of about 1 μm, and it is larger than sample II. Comparing the images of the three samples indicates that the sizes of the particles increased and the shape changed from nanoparticles into microflakes with an increase in irradiation time. All of the SAED patterns show a hexagonal structure, and the SAED pattern of samples II and III are much more ordered than that of sample I. The intensity and highly ordered diffraction spots mean that the particles are well crystallized, which is important for their use in high mobility-life solar cells.[27]

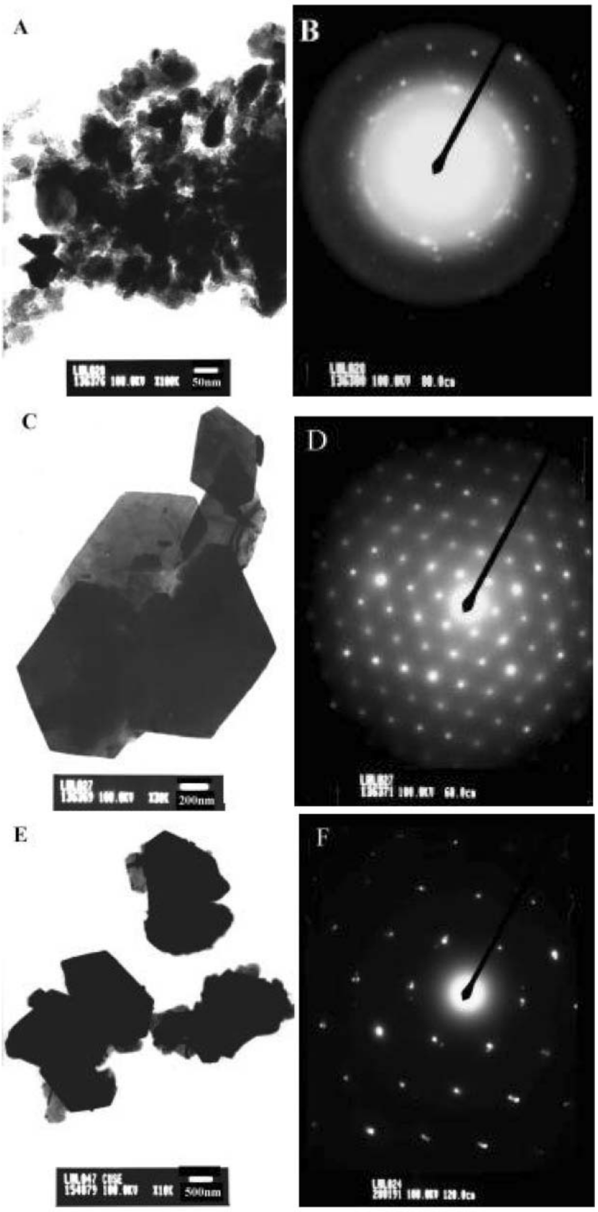

Fig. 3 TEM images and their SAED of the samples I (A, B), II (C, D) and III (E, F).

3.4 Thermal stability

A TGA measurement was conducted to characterize the thermal stability of the α-CuSe crystal. The typical TGA curve of sample I in the temperature range 25–1000 °C at a heating rate of 10 °C min^{-1} under Ar atmosphere exhibits one symmetric and drastic loss of weight at 440–480 °C (see ESI, Fig. S2†). This loss of weight is attributed to the decomposition of α-CuSe. The final decomposition product was confirmed to be Cu_2Se by XRD technique (JCPDS file No. 29-575), (Fig. 4). Furthermore, the amount of about 28% mass loss is in agreement with the theoretical value of 27.9% mass loss based on eqn. (1) for the production of Cu_2Se.

$$2CuSe \rightarrow Cu_2Se + Se \qquad (1)$$

The TGA result indicates that the as-prepared α-CuSe nanocrystals are stable below temperatures of 400 °C. This decomposition temperature is similar to the reported conversion temperature of CuSe to Cu_7Se_4 (at about 400 °C) for the chemical bath deposited CuSe film.[27] On the other hand, it also reveals that other kinds of copper selenide can be derived from the present α-CuSe crystal.

3.5 Optical properties

Copper selenides are well known as a *p*-type semiconductor possessing a direct band gap, as well as an indirect band gap.[44] However, their band gap value (E_g) varies with the change of their stoichiometries or phases. In order to understand the excitonic or interband (valence conduction band) transitions of α-CuSe, the DRS of the nanoparticle and flakes were measured. This allows us to calculate and determine their band gap. An estimate of the optical band gap is obtained using the following equations.[45]

$$\alpha(v) = A(h'v - E_g)^{m/2} \qquad (2)$$

where $h' = h/2\pi$, $h'v$ is the photon energy, α is the absorption coefficient, and m is dependent on the nature of the transition. For a direct transition, m is equal to 1 or 3, while for an indirect allowed transition, m is equal to 4 or 6. Since α is proportional to $F(R)$, the Kubelka–Munk function $F(R) = (1 - R)^2/2/R$, the energy intercept of a plot of $(F(R) \times hv)^2$ and $(F(R) \times hv)^{1/2}$ *versus* hv yields the $E_{g,dir}$ for a direct allowed transition and the $E_{g,ind}$ for an indirect allowed transition, respectively, when the linear regions are extrapolated to the zero ordinate. Using this method, similar indirect band gaps of about 1.31 eV are obtained for samples I and III (see ESI, Fig. S3†). This value is higher than the reported band gap of 1–1.1 eV of the bulk

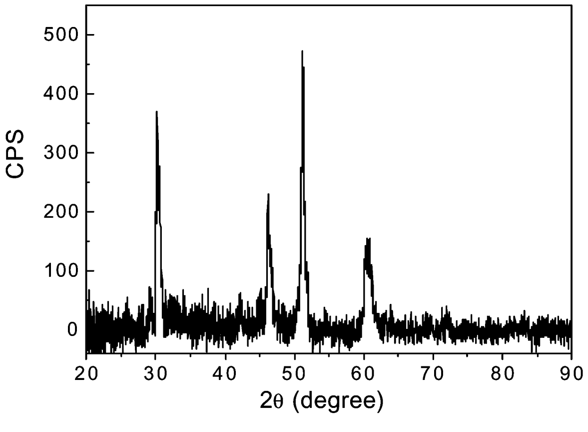

Fig. 4 XRD pattern of the resulting solid of the TGA measurement.

Cu_2Se,[46,47] and it is close to the reported indirect band gap 1.0–1.4 eV of $Cu_{2-x}Se$[44,48] and mineral klockmannite CuSe (JCPDS file No. 34-171).[27] Similar results were obtained if $(F(R) \times h\nu)^2$ is plotted against $h\nu$, as is appropriate for a direct semiconductor. For the present comparative exercise, we prefer the equation for an indirect semconductor according to the reported band gap values.

To obtain more information, photoacoustic spectra were applied to study the band gaps. In the present case, the PAS method was used for the measurements of the band gaps. Figs. 5(a) and (b) show the PA spectra of the nanoparticles and the flakes, respectively. For the nanoparticles, a direct band gap of about 2.39 eV was obtained. For the flakes, the direct band gap is about 2.21 eV. These results are close to the reported values of $Cu_{2-x}Se$[44,48,49] and mineral klockmannite CuSe nanoparticles prepared by chemical bath deposition methods,[27] which show band gaps of between 2.0 and 2.2 eV. The indirect band gaps are very close to the optimum value for solar cell application.[50] This means that the α-CuSe crystals produced by this method have potential applications as solar cell materials. To our knowledge, this is the first report of the optical properties of α-CuSe (JCPDS No. 6-427). Although there are a few reports on the optical properties of copper selenide families, their composition or phase is different from our samples. Both the direct band gap and the indirect band gap are higher as compared with the literature data of mineral klockmannite CuSe,[27] especially for the nanoparticles. This can be attributed to the quantization effect of the nanoparticles. The small quantization effect of sample III might originate from the third dimension confinement. However, it should be emphasized that no reliable data on the band gap of an α-CuSe single crystal is available in the literature for comparison, and therefore any explanation would be speculative.

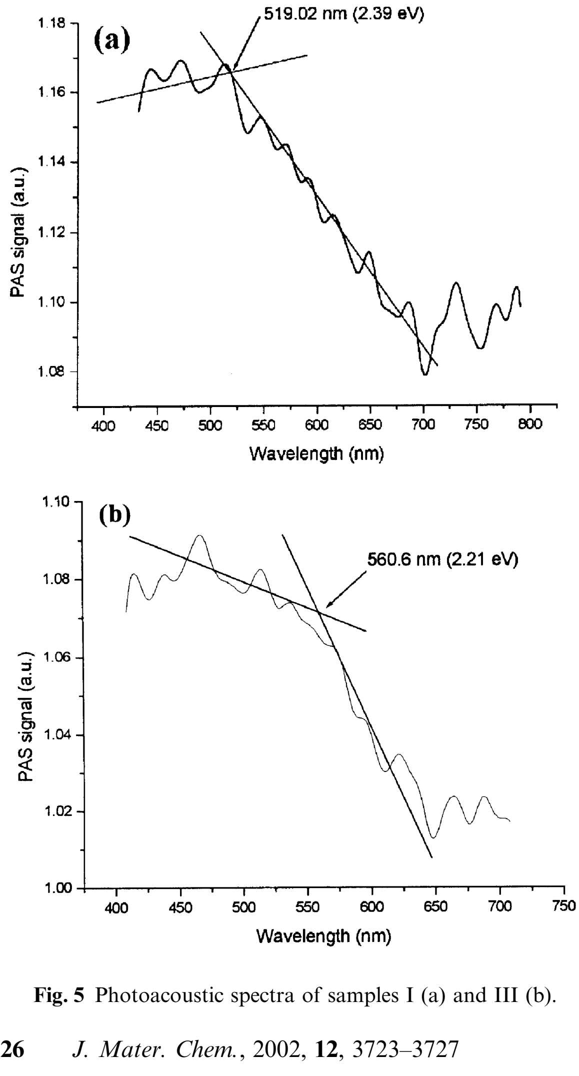

Fig. 5 Photoacoustic spectra of samples I (a) and III (b).

3.6 Reaction mechanism

Sonochemical reactions arise from acoustic cavitation phenomena: the formation, growth, and collapse of the bubbles in a liquid medium. The extremely high temperature (> 5000 K), pressure (> 20 Mpa), and cooling rates ($>10^{10}$ K s^{-1}) attained during acoustic cavitation lead to many unique properties in the irradiated solution.[51,52] The high temperatures and pressures produced in imploding cavitation bubbles lead to the thermal decomposition of water vapor or organic solvent vapor, forming radicals. The mechanism of the formation of CuSe takes into consideration the radical species from DMSO molecules by absorption of ultrasound [eqn. (3)].[53]

$$\text{DMSO)))) }{}^{\bullet}CH_3SO + {}^{\bullet}CH_3 \qquad (3)$$

The radicals formed in eqn. (3) can act as inducers and trigger the decomposition of excited $^{*}H_2$ molecule to $2H^{\bullet}$ [eqn. (4)].

$${}^{\bullet}CH_3 + {}^{*}H_2 \rightarrow CH_4 + H^{\bullet} \qquad (4)$$

The $H^{\bullet}$ react with Se in the high temperature interface region of the bubbles forming H_2Se [eqn. (5)].

$$E + 2H^{\bullet} \rightarrow H_2E\ (E = Se, S) \qquad (5)$$

The H_2E formed then reacts with Cu^{2+} *in situ*, forming the crystalline α-CuSe nanoparticles [eqn. (6)].

$$Cu^{2+} + H_2Se \text{)))) } CuSe + 2H^{+} \qquad (6)$$

A nanocrystalline product is expected if the reaction takes place at the interface of the bubbles.[54] On the other hand, an amorphous product is obtained if the reaction takes place inside the bubble as a result of the high cooling rates ($>10^{10}$ K s^{-1}) which occur during the collapse.[55] Therefore, it is assured that the reaction will take place at the interface, which explains the production of a well-crystallized product.

We have also considered and checked an alternative mechanism for the reaction. This possibility is that Cu^{2+} is reduced to elemental Cu during the first step because of the positive standard potential of Cu^{2+}/Cu, and the Cu then reacts with elemental Se during the next step. However, the control experiment indicates that H_2/Ar can not reduce Cu^{2+} to elemental Cu under ultrasound irradiation in DMSO (see section 3.1 XRD studies), while the DMSO can react with Cu^{2+} and form a complex. The formation of the complex in our experiment has been confirmed by FTIR results. It had also been clearly demonstrated that DMSO could react with some transition metal cations and form their coordinative compounds.[56,57] The formation of the coordinative compound between Cu^{2+} and DMSO reduces the reductive potential of Cu^{2+} to Cu. However, the complex still can react with the resulting H_2Se by releasing free Cu^{2+} homogeneously, forming high quality α-CuSe crystals (see section 3.1 XRD studies, Fig. 2). A similar function for NH_3 had been proposed in the preparation of CuSe nanoparticles by a hydrothermal method, with the assistance of NH_3.[58]

4 Conclusion

A sonochemical-assisted approach has been employed to prepare α-CuSe crystals. The size and the shape of the products can be affected by changing the reaction time. The α-CuSe crystals are stable below temperatures of about 480 °C. All of the crystals have an obvious absorption band in the visible region, with an indirect band gap of about 1.31 eV and a direct band gap of 2.2 eV for the flakes and 2.4 eV for the nanoparticles. The indirect band gap is very close to the optimum value for solar cell application. An ultrasound-assisted *in situ* reduction/reaction mechanism is proposed for the reaction. The role of DMSO in the reaction is not only that of a solvent but also that of a chelating reagent. This work also raises the possibility of creating other copper selenides or new ternary compounds using sonochemically prepared CuSe as a precursor.

Acknowledgements

H. L. Li thanks the Bar-Ilan Research Authority for a post-doctoral fellowship. Y. C. Zhu thanks the Kort 100 Scholarship Foundation for supporting his postdoctoral fellowship and also thanks the China Scholarship Council. A. Gedanken thanks the German Ministry of Science for the support of this work through the Deutche-Israeli DIP program. The authors are grateful to Prof. M. Deutsch, Department of Physics, and Ms. Judy, Department of Life Science, for extending the use of their facilities to us. We thank Dr. Shifra Hochberg and Mrs. Louise Braverman for editorial assistance. Kind assistance from Dr. V. Ganesh Kumar, Mr. G. Pol Vilas, and Mr. Menachem Motiei is gratefully acknowledged.

References

1 C. B. Murray, D. J. Norris and M. G. Bawendi, *J. Am. Chem. Soc.*, 1993, **115**, 8706.
2 T. Rajh, O. I. Micic and A. J. Nozik, *J Phys. Chem.*, 1993, **97**, 11999.
3 G. S. H. Lee, D. C. Graig, I. Ma, M. L. Scudder, T. D. Bailey and I. G. Dance, *J. Am. Chem. Soc.*, 1988, **110**, 4863.
4 N. Herron, J. C. Calabrese, W. E. Farneth and Y. Wang, *Science*, 1993, **259**, 1426.
5 T. Vossmeyer, G. Reck, L. Katsikas, E. T. K. Haupt, B. Schulz and H. Wells, *Science*, 1995, **267**, 1476.
6 J. J. Zhu, O. Palchik, S. G. Chen and A. Gedanken, *J. Phys. Chem. B*, 2000, **104**, 7344.
7 J. J. Zhu, Y. Koltypin and A. Gedanken, *Chem. Mater.*, 2000, **12**, 73.
8 H. C. Yi and J. J. Moore, *J. Mater. Sci.*, 1990, **25**, 1159.
9 D. M. Wilhemg and E. Matijevic, *J. Chem. Soc. Faraday Trans*, 1984, **1**, 563.
10 N. L. Pickett, D. F. Forster and D. L. Gole, *J. Mater. Chem.*, 1996, **6**, 507.
11 Y. Wang and N. Herron, *J. Phys. Chem.*, 1987, **91**, 257.
12 A. R. Korton, R. Hull, R. L. Opita, M. G. Bawendi, M. L. Steigerword, P. J. Carroll and L. E. Brus, *J. Am. Chem. Soc.*, 1990, **112**, 1327.
13 V. Sankaran, C. C. Cummings, R. R. Schrock, R. E. Cohen and R. J. Silby, *J. Am. Chem. Soc.*, 1990, **112**, 6858.
14 J. C. Luong, *Superlattices Microstruct.*, 1996, **8**, 161.
15 M. Stoev and A. Katerski, *Chem. Mater.*, 1996, **6**, 377.
16 I. P. Parki, *Chem. Soc. Rev.*, 1996, **25**, 199.
17 V. Dusastre, B. Omar, I. P. Parkin and G. A. Shaw, *J. Chem. Soc., Dalton Trans.*, 1997, 3505.
18 W. X. Zhang, X. M. Zhang, L. Zhang, J. X. Wu, Z. H. Hui, Y. W. Chang, J. W. Liu, Y. Xie and Y. T. Qian, *Inorg. Chem.*, 2000, **39**, 1838.
19 J. Yang, G. H. Chang, J. H. Zeng, S. H. Yu, X. M. Liu and Y. T. Qian, *Chem. Mater.*, 2001, **13**, 848.
20 B. Li, Y. Xie, J. X. Huang and Y. T. Qian, *Inorg. Chem.*, 2001, **39**, 2061.
21 B. Li, Y. Xie, J. X. Huang, Y. Liu and Y. T. Qian, *Chem. Mater.*, 2000, **12**, 2614.
22 S. T. Lakshmikvmar, *Mater. Solar Cells*, 1994, **32**, 7.
23 H. Toyoji and Y. Hiroshi, *Jpn. Kokai Tokkyo Koho*, 1990, JP 02 173–622.
24 A. A. Korzhuev, *Fiz Kihm Obrab Mater.*, 1991, **3**, 131.
25 A. Oshitasi, *Jpn. Kokai Tokkyo Koho,* JP 61 222–911.
26 T. Ohtani and M. Motoki, *Mater. Res. Bull.*, 1995, **30**, 1495.
27 V. M. Garcia, P. K. Nair and M. T. S. Nair, *J. Cryst. Growth*, 1999, **203**, 113.
28 *Powder Diffraction File, Inorganic Phases, Alphabetical Index*, JCPDS, PA, 1985, p. 264 and p. 671.
29 A. L. N. Stevels and F. Jellinek, *Recueil*, 1971, **111**, 273.
30 R. D. Heyding, *Can. J. Chem.*, 1996, **44**, 1233.
31 A. Schafer, M. Kouwitz and R. Ahlrichs, *J. Chem. Phys.*, 1996, **104**, 7113.
32 W. Z. Wang, P. Yan, F. Y. Liu, Y. Xie, Y. Geng and Y. T. Qian, *J. Mater. Chem.*, 1998, **8**, 2321.
33 Z. H. Han, Y. P. Li, H. Q. Zhao, S. H. Yu, X. L. Yin and Y. T. Qian, *Mater. Lett.*, 2000, **44**, 366.
34 H. L. Su, Y. Xie, Z. P. Qiao and Y. T. Qian, *Mater. Res. Bull.*, 2000, **35**, 1129.
35 A. Henglein, *Ultrasonics*, 1987, **25**, 6.
36 K. S. Suslick, S. J. Doktycz and E. B. Flint, *Ultrasonics*, 1990, **28**, 280.
37 *Ultrasound; Its Chemical, Physical and Biological Effect*, ed. K. S. Suslick, VCH, Weinheim, 1988.
38 K. S. Suslick, S. B. Choe, A. A. Cichowlas and M. W. Grinstaff, *Nature*, 1991, **353**, 414.
39 N. Dhas and A. Gedanken, *J. Phys. Chem. B*, 1997, **101**, 9495.
40 W. Y. Wang, X. H. Tang, L. X. Yin, W. P. Huang, Y. R. Hacohen and A. Gedanken, *Adv. Mater.*, 2000, **12**, 1183.
41 S. Avivi, Y. Mastai, G. Hodes and A. Gedanken, *J. Am. Chem. Soc.*, 1999, **121**, 4196.
42 M. A. Slifkin, L. Luria and A. M. Weiss, *SPIE-Int. Soc. Opt. Eng.*, 1998, **3110**, 481.
43 A. Rosencwaig, *Photoacoustics and photoacoustic spectroscopy*, Academic, New York, 1980.
44 A. M. Hermann and L. Fabick, *J. Cryst. Growth*, 1983, **61**, 658.
45 V. Luca, S. Djajanti and R. F. Howe, *J. Phys. Chem. B*, 1998, **102**, 10650.
46 *Landolt-Bornstein, Numerical Data and Functional Relationships in Science and Technology, New Series, Group III*, ed. Hellwege, Springer, Berlin, 1983, vol. 17e.
47 O. Madelung, *Semiconductors, Other than Group IV Elements and III–V Compounds*, Springer, Berlin, 1992, p. 51.
48 K. L. Chopra and S. R. Das, *Thin Film Solar Cells*, Plenum, New York, 1983.
49 A. Mondal and P. Pramanik, *J. Solid State Chem.*, 1983, **47**, 81.
50 J. J. Loferski, *J. Appl. Phys.*, 1956, **27**, 777.
51 K. S. Suslick, D. A. Hammerton and R. E. Cline, *J. Am. Chem. Soc.*, 1986, **108**, 564.
52 K. S. Suslick and D. A. Hammerton, *IEEE Trans. Ultrason., Ferrelec., Freq. Contrl*, 1986, **33**, 143.
53 T. Kondo, L. J. Kirschenbaum, H. Kim and P. Riese, *J. Phys. Chem.*, 1993, **97**, 522.
54 P. Jeevanandam, Y. Koltypin, A. Gedanken and Y. Mastai, *J. Mater. Chem.*, 2000, **10**, 511.
55 W. B. McNamara III, Y. T. Didenko and K. S. Suslick, *Nature*, 1999, **401**, 772.
56 B. J. Coe, T. J. Meyer and P. S. White, *Inorg. Chem.*, 1995, **34**, 593.
57 S. Alkaradaghi, E. S. Cedergrenzeppezauer, Z. Dauter and K. S. Wilson, *Acta Crystallogr., Sect. D: Biol. Crystallogr.*, 1995, **51**, 805.
58 H. L. Su, Y. Xie and Y. T. Qian, *Mater. Res. Bull.*, 2000, **35**, 465.